Acta Oceanol. Sin., 2020, Vol. 39, No. 2, P. 12–21
https://doi.org/10.1007/s13131-020-1550-z
http://www.hyxb.org.cn
E-mail: hyxbe@263.net

Distribution patterns of ^{210}Po, ^{210}Pb and the particle export in the Taiwan Strait during the winter

Lihao Zhang[1, 2], Weifeng Yang[2]*, Min Chen[2], Yinian Zhu[1]*, Zhou Wang[2], Ziming Fang[2], Yusheng Qiu[2], Yanhong Li[1]

[1] Guangxi Key Laboratory of Environmental Pollution Control Theory and Technology, Guilin University of Technology, Guilin 541004, China

[2] State Key Laboratory of Marine Environmental Science/College of Ocean and Earth Sciences, Xiamen University, Xiamen 361102, China

Received 5 November 2018; accepted 19 February 2019

Abstract

^{210}Po and ^{210}Pb are increasingly used to constrain particle dynamics in the open oceans, however they are less used in coastal waters. Here, distributions and partitions of ^{210}Po and ^{210}Pb were examined in the Taiwan Strait, as well as their application to quantify particle sinking. Activity concentrations of dissolved ^{210}Po and ^{210}Pb (<0.6 μm) ranged from 1.21 to 7.63 dpm/(100 L) and from 1.07 to 6.33 dpm/(100 L), respectively. Activity concentrations of particulate ^{210}Po and ^{210}Pb varied from 1.96 to 36.74 dpm/(100 L) and from 3.11 to 38.06 dpm/(100 L). Overall, particulate ^{210}Po and ^{210}Pb accounted for the majority of the bulk ^{210}Po and ^{210}Pb. ^{210}Po either in dissolved or particulate phases showed similar spatial patterns to ^{210}Pb, indicating similar mechanisms for controlling the distributions of ^{210}Po and ^{210}Pb in the Taiwan Strait. The different fractionation coefficients indicated that particles in the Zhemin Coastal Current (ZCC) inclined to absorb ^{210}Po prior to ^{210}Pb while they showed an opposite effect in the Taiwan Warm Current (TWC). Based on the disequilibria between ^{210}Po and ^{210}Pb, the sinking fluxes of total particulate matter (TPM) were estimated to range from –0.22 to 3.84 g/(m^2·d), showing an overall comparable spatial distribution to previous reported sediment accumulation rates. However, our sinking fluxes were lower than the sedimentation rates, indicating a sediment resuspension in winter and horizontal transport of particulate matter from the Taiwan Strait to the East China Sea.

Key words: Taiwan Strait, ^{210}Po, ^{210}Pb, resuspension, export flux, sedimentation

Citation: Zhang Lihao, Yang Weifeng, Chen Min, Zhu Yinian, Wang Zhou, Fang Ziming, Qiu Yusheng, Li Yanhong. 2020. Distribution patterns of ^{210}Po, ^{210}Pb and the particle export in the Taiwan Strait during the winter. Acta Oceanologica Sinica, 39(2): 12–21, doi: 10.1007/s13131-020-1550-z

1 Introduction

The Taiwan Strait is located in the southeast of China and its current system is significantly affected by the East Asian monsoon (Sun, 2016). In summer and winter, northeast and southwest monsoons prevail respectively. In the west of Taiwan Strait, several rivers, i.e., Oujiang River, Minjiang River and Jiulong River, input an amount of nutrients to the Taiwan Strait with low temperature and low salinity water (Shang et al., 2001; Xiao et al., 2002). The Zhemin Coastal Current (ZCC), flowing from the East China Sea (ECS) to the Taiwan Strait along the coastline, plays an important role in regulating the current system and ocean productivity in the Taiwan Strait (Hu et al., 1999; Xiao et al., 2002). Meanwhile, a large amount of biogenic particles produced in the ECS get into the strait along with the ZCC. In addition, the warm current, flowing from the Taiwan Strait to the ECS (Huh and Su, 1999), probably transports particles produced in the middle strait to the continental shelf of the ECS. Thus, the Taiwan Strait is an important area for our understanding of the material budget in both the ECS and South China Sea (Hu et al., 2010).

Due to the interactions among the Taiwan Strait branch of Kuroshio, South China Sea Warm Current (SCSWC) and ZCC, the biogeochemical processes in the Taiwan Strait showed large variability over weekly to seasonal timescales. Radionuclides with half-lives matching these timescales would provide insights into the geochemical processes. In this study, ^{210}Po ($T_{1/2}$=138.4 d) and ^{210}Pb ($T_{1/2}$=22.3 a) were used to constrain the particle dynamics in the Taiwan Strait. Naturally occurring ^{210}Po and ^{210}Pb are both particle reactive radionuclides of ^{238}U decay series, and ^{210}Po is produced from the decay of ^{210}Pb through ^{210}Bi (Moore et al., 1973). Recently, ^{210}Po and ^{210}Pb have been widely utilized to study the kinetics of particle cycling and export flux of particle organic carbon in oceans (Chen et al., 2012; Fang et al., 2013; Wei et al., 2011; Yang et al., 2011). Though ^{210}Po and ^{210}Pb are particle-active, there is difference between them during adsorbing onto particles. ^{210}Po is easier to be absorbed onto biogenic particles than ^{210}Pb and get involved into the biogeochemical cycling (Nozaki et al., 1997; Fisher et al., 1987; Fowler, 2011; Yang et al., 2013, 2015). In general, the disequilibrium between ^{210}Po and ^{210}Pb is prevalent in the biogeochemical cycling processes.

In marine environments, particle sinking depends on hydro-

Foundation item: The National Natural Science Foundation of China under contract Nos 41076043 and 51608142; the Guangxi Young and Middle-aged Teachers' Basic Ability Upgrading Project under contract No. 2019KY0298; the Guangxi Science and Technology Planning Project under contract No. GuiKe-AD18126018.
*Corresponding author, E-mail: wyang@xmu.edu.cn; zhuyinian@glut.edu.cn

dynamic conditions, physicochemical and biological processes (Xu and Chen, 1999). In the west of Taiwan Strait, sediments usually have high sand content with respect to the southward shale muddy and riverine particles (Zhou, 1987). In the north of Taiwan Strait, currents often introduce sediment resuspension (Wang et al., 2014a). A few reports used ^{210}Pb to study the sedimentation patterns of particle in the last century in the Taiwan Strait (Huh et al., 2011). Li et al. (2015) reported that small river plume could affect the along-strait or cross-strait transport of total particulate matter (TPM) in the western Taiwan Strait. However, the sinking of particles within the Taiwan Strait and their influence on the mass balance of sediments in the strait are poorly understood. In addition, the seasonal variability in the fate of particulate matters is rarely reported in the Taiwan Strait. In this study, the disequilibria between ^{210}Po and ^{210}Pb in the northwestern Taiwan Strait during winter were examined as well as the particle dynamics. Moreover, the sinking fluxes of ^{210}Po and TPM were quantified to provide insights into the seasonal fate of particles in the Taiwan Strait.

2 Methods

2.1 *Sampling*

Seawater samples were collected onboard R/V *Yanping II* during the winter cruise in the northwestern Taiwan Strait from January 3 to February 22, 2012. Sampling stations were shown in Fig. 1. About 5 L seawater was collected using the CTD rosette system and filtered immediately on board through PC Millipore membrane filters to separate particulate from dissolved phase (<0.6 μm). Filters containing particulate matter were put into precleaned plastic bags and then stored at –18°C before analysis. Dissolved fraction (~5 L) was transferred into a clean polyethylene bottle and acidified with concentrated HCl to pH<2 for analysis in the land laboratory.

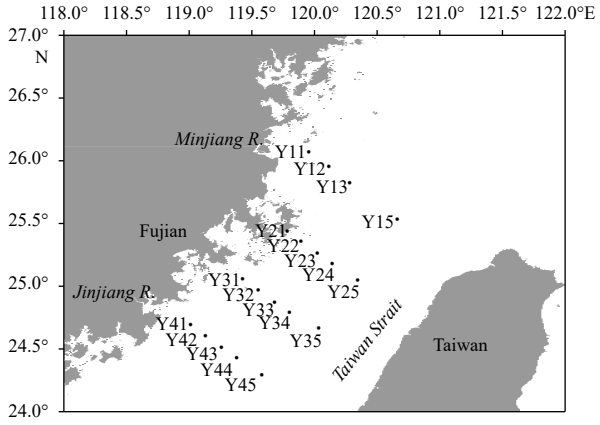

Fig. 1. Sampling locations in the Taiwan Strait in February 2012.

2.2 *^{210}Po, ^{210}Pb and TPM analysis*

The filter membranes containing particulate matter were dried at 60°C and weighed to a constant weight. TPM contents were calculated based on the difference in the weight between particle-contained dry membrane and pre-filtered membrane.

The activity concentrations of ^{210}Po and ^{210}Pb in dissolved and particulate phases were determined following the procedures described by Yang et al. (2013) and Zhang (2015). Briefly, 3.13 mg Pb^{2+}, quantitative spike of ^{209}Po and icon carrier ($FeCl_3$) were added into the filtrate while stirring. After 8 h for isotopic equilibration, the solution was adjusted to a pH value of 9 with ammonia solution to form $Fe(OH)_3$ precipitates. The $Fe(OH)_3$ precipitates were collected by siphoning and centrifuging, and then re-dissolved with 6 mol/L HCl. Then the solution was transferred into a 100 mL Teflon beaker. After adjusting pH to about 1.5, ascorbic acid for sheltering Fe^{3+}, 2 mL of 25% sodium citrate and 2 mL of 25% hydroxylamine hydrochloride were added, and then the pH value was adjusted to 1.5–2.0. Po isotopes were deposited on a silver disc through a magnetic stirrer at 85–90°C for about 4 h. The silver disc was rinsed with Milli-Q water and dried naturally. Activities of ^{209}Po and ^{210}Po on the disc were measured using an alpha spectrometer (Octéte^{TM} PC, EG&G). For particulate samples, particles were digested with HNO_3 and $HClO_4$. The auto-deposition and measurements of Po were the same as dissolved samples. Solution after Po deposition was preserved for more than 1 year to determine the activity of ^{210}Pb via its daughter ^{210}Po. In this study, sampling date and time, reagent blanks, instrument backgrounds, decay, ingrowth and error propagation were corrected on the base of ±1σ counting errors (Yang, 2005; Zhang, 2015).

2.3 *Partition and fractionation coefficient*

The partition coefficient (K_d) of nuclides between dissolved and particulate phases could be applied to explain the difference of nuclides in distribution between solid and liquid phases, and it is calculated using the following equation (Wei et al., 2012; Jones et al., 2015):

$$K_d = PA/(DA \times TPM), \quad (1)$$

where DA and PA denote the activities of dissolved and particulate nuclides respectively, and TPM represents the concentration of the total particulate matter. The calculated partition coefficients were shown in Table 1.

Based on the partition coefficients of nuclides, the fractionation coefficient (α) were calculated via K_d and presented in Table 1.

$$\alpha = K_{d,\,Po}/K_{d,\,Pb}. \quad (2)$$

3 Results

3.1 *Temperature and salinity*

During the cruise, temperature and salinity of the seawater in the western Taiwan Strait ranged from 9.1°C to 20.6°C and from 29.8 to 34.4 (n=67), respectively. The spatial distributions were shown in Fig. 2. These parameters indicated that the main current with low temperature and salinity in the western Taiwan Strait is the ZCC. This current, affected by the topography, played a role in the exchange of material between the Fujian coast and the middle strait. Within the upper 30 m, the ZCC paralleled to the coastline. Seawater with high temperature and salinity dominated the mid-strait from the south to north (Hu et al., 1999), representing the Kuroshio branch from the Luzon Strait joint to the SCSWC in the Taiwan Strait and formed the Taiwan Warm Current (TWC) (Xiao et al., 2002; Shang et al., 2001; Hu et al., 2010) . A clear front was observed between the ZCC and the TWC (Fig. 2).

3.2 *Activity concentrations of ^{210}Po and ^{210}Pb*

Activity concentrations of ^{210}Po and ^{210}Pb were presented in Table 1 and their distributions were presented in Fig. 3. D^{210}Po

Table 1. Sampling stations, temperature, salinity, activity concentrations of ^{210}Po and ^{210}Pb in seawater, and K_d values for ^{210}Po and ^{210}Pb and TPM concentrations in the Taiwan Strait in February 2012

Sample ID	Layer depth/m	T/°C	S	$D^{210}Po$ /dpm·(100 L)$^{-1}$	$D^{210}Pb$ /dpm·(100 L)$^{-1}$	$P^{210}Po$ /dpm·(100 L)$^{-1}$	$P^{210}Pb$ /dpm·(100 L)$^{-1}$	TPM/mg·L^{-1}	$K_{d,Po}$ /L·mg^{-1}	$K_{d,Pb}$ /L·mg^{-1}	α
Y41	3	11.46	30.52	6.29±0.41	3.59±0.46	3.84±0.38	9.53±0.94	3.31	0.18±0.04	0.80±0.05	0.23±0.05
	10	10.98	30.52	2.26±0.19	2.33±0.39	4.42±0.44	10.67±0.98	4.96	0.39±0.03	0.92±0.04	0.42±0.04
	20	11.14	31.32	2.27±0.22	6.02±0.74	7.97±0.73	28.21±2.59	7.73	0.45±0.02	0.61±0.02	0.74±0.04
	35	11.72	31.73	2.01±0.19	5.97±0.71	9.91±0.80	14.29±1.25	11.61	0.42±0.01	0.21±0.01	2.00±0.11
Y42	3	11.90	31.24	2.68±0.24	6.28±0.82	5.42±0.53	9.36±0.79	3.81	0.53±0.04	0.39±0.04	1.36±0.17
	10	11.13	31.29	3.09±0.23	5.45±0.62	3.94±0.42	7.29±0.66	3.25	0.39±0.04	0.41±0.04	0.95±0.13
	20	11.28	31.39	2.51±0.20	4.11±0.46	4.04±0.37	5.45±0.50	3.64	0.44±0.03	0.36±0.04	1.22±0.16
	30	12.42	32.09	4.61±0.29	4.21±0.47	6.73±0.44	7.97±0.70	6.22	0.23±0.01	0.30±0.02	0.77±0.06
	50	12.87	32.30	6.44±0.43	4.25±0.46	10.05±0.69	17.88±1.68	8.62	0.18±0.01	0.49±0.02	0.37±0.03
Y43	3	12.73	31.95	2.13±0.21	3.46±0.43	3.75±0.34	5.07±0.55	1.86	0.95±0.07	0.79±0.09	1.20±0.16
	10	12.62	32.05	2.36±0.22	4.04±0.46	4.58±0.50	10.42±1.02	2.63	0.74±0.05	0.98±0.06	0.76±0.07
	30	12.50	32.15	2.18±0.19	2.35±0.31	4.45±0.41	9.40±0.90	3.62	0.56±0.03	1.11±0.04	0.50±0.03
	50	15.93	33.57	3.17±0.27	3.36±0.37	7.03±0.50	16.36±1.62	3.46	0.64±0.03	1.41±0.04	0.45±0.02
	59	15.97	33.58	2.95±0.24	3.11±0.43	6.60±0.52	10.88±1.05	3.55	0.63±0.03	0.99±0.05	0.64±0.04
Y44	3	14.04	32.79	2.53±0.21	2.56±0.33	4.51±0.40	25.60±2.79	1.04	1.71±0.11	9.59±0.16	0.18±0.01
	10	13.78	32.80	2.45±0.21	6.33±0.76	2.73±0.28	6.29±0.66	1.10	1.01±0.12	0.90±0.14	1.12±0.22
	30	15.41	33.40	2.57±0.21	3.66±0.49	3.69±0.32	3.71±0.37	1.51	0.95±0.08	0.67±0.11	1.42±0.26
	50	15.16	33.37	2.62±0.21	3.21±0.42	7.22±0.49	7.60±0.73	3.82	0.72±0.03	0.62±0.04	1.16±0.09
	65	13.98	33.18	3.03±0.28	3.04±0.30	15.53±1.19	18.19±1.50	10.07	0.51±0.01	0.59±0.01	0.86±0.02
Y45	3	20.62	33.98	7.63±0.58	4.69±0.47	4.18±0.35	3.11±0.36	1.29	0.43±0.09	0.52±0.12	0.83±0.26
	10	20.63	33.98	3.71±0.30	2.18±0.20	3.36±0.29	5.24±0.53	1.17	0.77±0.10	2.06±0.12	0.37±0.05
	28	20.62	33.97	4.44±0.39	3.38±0.32	4.35±0.40	8.40±0.93	1.84	0.53±0.07	1.35±0.08	0.39±0.06
Y31	3	10.29	30.66	1.64±0.18	1.88±0.30	6.59±0.58	7.53±0.77	2.00	0.64±0.02	0.64±0.03	1.00±0.06
	10	10.11	30.71	1.45±0.17	2.27±0.31	18.78±1.57	19.23±2.22	10.57	0.67±0.01	0.44±0.01	1.52±0.04
	20	10.16	30.87	2.38±0.27	2.32±0.31	20.78±1.61	26.27±2.96	3.62	0.30±0.01	0.39±0.01	0.77±0.03
Y32	3	10.98	31.22	1.80±0.17	2.59±0.31	2.75±0.32	3.96±0.39	1.62	0.53±0.05	0.53±0.05	1.00±0.13
	20	10.90	31.22	1.67±0.18	2.40±0.31	6.41±0.52	6.86±0.63	2.05	0.69±0.02	0.51±0.03	1.35±0.09
	40	12.61	32.07	2.51±0.24	2.91±0.48	36.74±3.16	38.06±3.44	1.63	0.44±0.01	0.40±0.01	1.10±0.04
Y33	3	11.12	31.34	1.33±0.15	3.13±0.41	2.79±0.31	6.17±0.61	3.70	0.69±0.05	0.65±0.05	1.06±0.11
	20	11.17	31.58	1.50±0.22	2.45±0.33	4.88±0.49	5.52±0.57	12.75	0.88±0.05	0.61±0.05	1.44±0.14
	50	14.03	33.01	3.34±0.38	3.68±0.57	22.24±1.68	18.69±1.91	14.22	0.52±0.01	0.40±0.01	1.30±0.04
	70	13.98	33.02	2.16±0.26	2.89±0.42	24.35±2.01	18.81±1.58	0.76	0.79±0.01	0.46±0.01	1.72±0.04
Y34	3	13.73	32.63	2.12±0.22	1.58±0.30	3.34±0.41	6.19±0.60	5.58	2.09±0.21	5.18±0.28	0.40±0.05
	20	14.21	33.05	2.17±0.22	2.27±0.28	4.95±0.46	13.14±1.15	32.89	1.41±0.08	3.57±0.09	0.39±0.02
	55	14.17	33.07	4.03±0.35	3.78±0.60	4.57±0.53	7.34±0.65	3.04	0.55±0.07	0.95±0.09	0.58±0.09
Y35	3	13.08	32.25	2.38±0.21	1.89±0.29	1.96±0.26	3.12±0.34	6.24	0.50±0.10	1.01±0.12	0.50±0.12
	20	12.70	32.29	1.96±0.17	1.58±0.36	3.72±0.34	4.50±0.44	19.35	0.95±0.06	1.42±0.12	0.67±0.07
	50	12.66	32.29	2.22±0.24	3.06±0.41	4.87±0.41	8.56±0.92	29.12	0.21±0.01	0.26±0.02	0.81±0.07
	59	12.66	32.29	1.72±0.19	1.07±0.17	–	–	2.90	–	–	–
Y21	3	9.89	30.01	2.32±0.40	2.97±0.40	11.27±1.11	7.19±0.65	6.83	0.41±0.02	0.21±0.01	1.95±0.13
	10	9.95	30.17	1.21±0.24	1.61±0.20	20.97±1.79	8.86±1.01	12.61	1.01±0.01	0.32±0.01	3.16±0.10
	16	9.95	30.46	2.12±0.31	2.65±0.32	8.41±1.22	14.79±1.71	1.55	0.16±0.01	0.22±0.01	0.73±0.06
Y22	3	10.20	29.88	1.55±0.26	1.87±0.23	23.50±2.31	12.74±1.17	1.44	2.03±0.03	0.91±0.02	2.23±0.06
	20	10.00	30.66	1.37±0.23	1.50±0.28	11.88±0.97	11.08±1.06	7.84	1.13±0.02	0.96±0.03	1.18±0.04
	41	11.45	32.63	1.42±0.24	1.98±0.26	15.89±1.34	23.20±2.10	10.63	0.46±0.01	0.48±0.01	0.96±0.03
Y23	3	10.65	30.52	1.79±0.29	2.44±0.28	3.10±0.43	4.01±0.41	5.48	0.73±0.09	0.69±0.07	1.06±0.17
	20	12.22	32.06	1.58±0.28	1.95±0.27	5.52±0.67	5.02±0.48	23.72	0.64±0.04	0.47±0.03	1.36±0.12
	30	13.74	32.89	2.19±0.42	2.29±0.30	24.61±2.39	21.70±2.35	2.12	0.47±0.01	0.40±0.01	1.18±0.04
Y24	3	11.12	31.27	1.80±0.30	1.93±0.25	3.65±0.42	7.36±0.68	7.66	0.96±0.10	1.80±0.08	0.53±0.06
	20	11.39	31.75	1.21±0.23	2.03±0.26	4.37±0.54	5.85±0.56	24.23	0.81±0.05	0.65±0.04	1.25±0.11
	48	13.36	32.83	2.54±0.41	2.69±0.35	20.07±1.74	30.43±3.27	2.37	0.38±0.01	0.54±0.01	0.70±0.02
Y25	3	12.32	31.85	2.21±0.25	3.37±0.42	4.30±0.61	5.78±0.56	11.70	1.11±0.10	0.98±0.09	1.13±0.15
	20	12.74	32.33	2.08±0.21	2.30±0.29	4.35±0.54	4.86±0.47	17.13	1.72±0.13	1.75±0.13	0.98±0.10
	50	12.47	32.82	2.22±0.32	1.91±0.28	14.89±1.37	13.98±1.32	25.43	0.66±0.02	0.72±0.02	0.92±0.04

to be continued

Continued from Table 1

Sample ID	Layer depth/m	T/°C	S	$D^{210}Po$	$D^{210}Pb$	$P^{210}Po$	$P^{210}Pb$	TPM/mg·L^{-1}	$K_{d,Po}$	$K_{d,Pb}$	α
				/dpm·(100 L)$^{-1}$					/L·mg^{-1}		
	64	12.02	32.95	2.14±0.33	2.89±0.35	32.48±3.11	28.02±2.91	7.46	0.65±0.01	0.41±0.01	1.59±0.05
Y11	3	9.17	29.76	1.32±0.27	1.86±0.27	5.92±0.71	33.43±3.31	4.46	0.12±0.01	0.50±0.01	0.24±0.02
	10	9.06	29.96	1.44±0.29	1.95±0.28	10.12±1.44	16.30±1.30	21.06	0.22±0.01	0.27±0.01	0.81±0.05
	25	9.31	30.68	1.55±0.30	2.06±0.29	17.79±1.93	19.54±1.69	1.75	0.44±0.01	0.36±0.01	1.22±0.04
Y12	3	10.57	32.34	1.55±0.30	1.87±0.28	6.99±0.96	14.07±1.27	1.21	0.44±0.02	0.74±0.02	0.59±0.03
	20	10.49	32.35	1.83±0.34	1.64±0.25	7.84±0.93	18.86±1.76	10.14	0.29±0.01	0.77±0.01	0.38±0.01
	40	10.49	32.39	1.60±0.29	2.47±0.29	12.87±1.39	10.08±1.03	23.42	0.97±0.03	0.49±0.02	1.98±0.10
Y13	3	13.83	34.34	1.39±0.28	1.94±0.26	13.32±2.37	14.05±1.49	35.84	0.47±0.01	0.35±0.01	1.34±0.05
	20	13.83	34.34	1.25±0.23	1.77±0.23	2.50±0.49	5.94±0.68	31.21	0.29±0.04	0.49±0.03	0.59±0.09
	48	13.82	34.33	1.79±0.31	3.49±0.37	8.53±0.83	21.11±1.83	26.38	0.38±0.02	0.48±0.01	0.79±0.04
Y15	10	13.18	32.89	2.28±0.33	2.79±0.32	14.23±1.42	19.57±2.25	10.14	4.03±0.11	4.54±0.10	0.89±0.03
	20	13.19	32.89	4.13±0.73	3.84±0.47	6.86±1.19	5.63±0.56	14.87	1.15±0.17	1.02±0.11	1.13±0.21
	50	14.11	34.31	1.95±0.35	2.37±0.34	7.74±1.04	9.09±0.80	8.32	0.51±0.03	0.49±0.02	1.04±0.07
	75	14.19	34.35	1.63±0.25	1.89±0.22	14.69±1.37	16.97±2.00	20.56	0.85±0.02	0.84±0.02	1.01±0.03

Note: – means no data. $D^{210}Po$ and $D^{210}Pb$ represent activity concentrations of dissolved ^{210}Po and ^{210}Pb, respectively. $P^{210}Po$ and $P^{210}Pb$ represent activity concentrations of particulate ^{210}Po and ^{210}Pb, respectively.

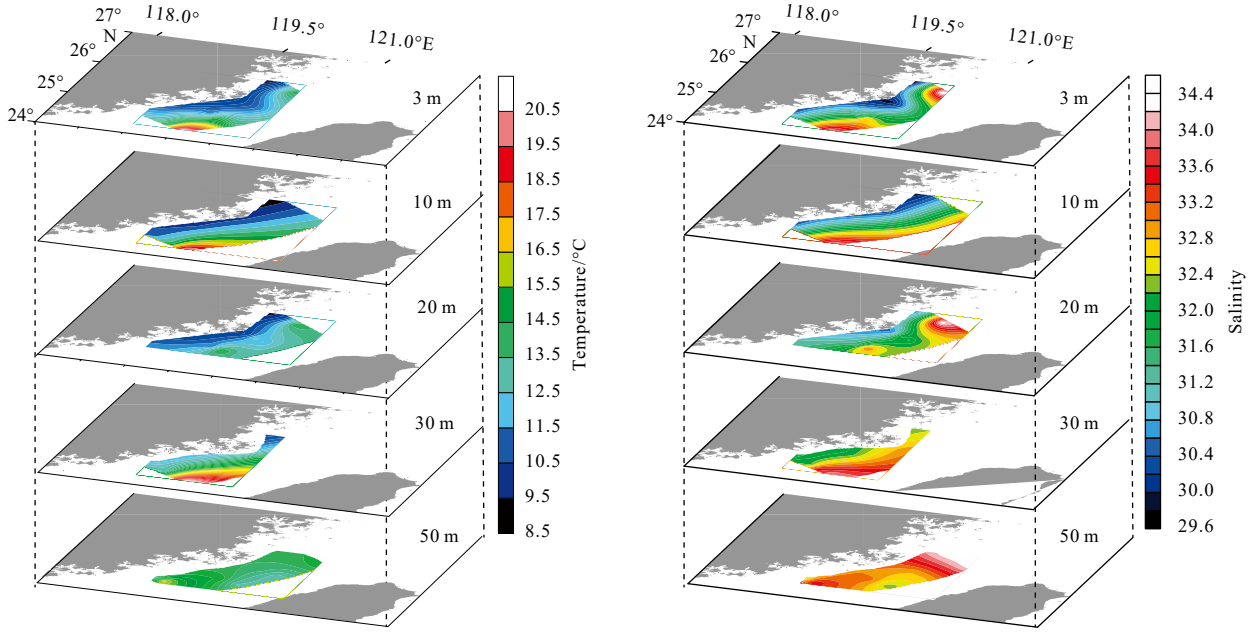

Fig. 2. Distributions of temperature and salinity in the Taiwan Strait in February 2012.

activity concentrations ranged from 1.21 to 7.63 dpm/(100 L) with the average of 2.41 dpm/(100 L), comparable to the value obtained in the Taiwan Strait (Wei et al., 2015). In the ZCC, $D^{210}Po$ activity concentrations were low and increased gradually from the Fujian coast to the central strait. In addition, $D^{210}Po$ gradually decreased from the south to north in the TWC, indicating the influence of the warm current (Wei et al., 2009; Wei et al., 2015). The TWC from the South China Sea and Kuroshio usually has higher $D^{210}Po$ due to its low biological productivity and scare particles (Yang et al., 2006). $P^{210}Po$ activity concentrations varied from 1.96 to 36.74 dpm/(100 L) (averaging 9.50 dpm/(100 L)) with the highest value near the coast. The distribution pattern of the total ^{210}Po (D+P) was similar to $P^{210}Po$, corresponding to the major contribution of $P^{210}Po$ to the total ^{210}Po pool.

$D^{210}Pb$ activity concentrations varied from 1.07 to 6.33 dpm/(100 L) with a mean value of 2.88 dpm/(100 L) (Fig. 4). Overall, the distribution of $D^{210}Pb$ showed a similar pattern to that of $D^{210}Po$. In the upper 30 m, the lowest concentration was observed in the northwest strait, indicating the influence of the ZCC. $D^{210}Pb$ activity concentrations in the southern strait were higher than those observed in the northern strait. Similarly, $P^{210}Pb$ showed high activity concentrations at the nearshore stations as $P^{210}Po$.

The distributions of the total ^{210}Po ($T^{210}Po$) and ^{210}Pb (D+P) were presented in Fig. 5. There is a similarity between $T^{210}Po$ and $P^{210}Po$, corresponding to the higher percentages of $P^{210}Po$ in $T^{210}Po$ in northwestern strait in winter (Table 1). About 77% of $T^{210}Pb$ was in the particulate form, comparable to $P^{210}Po$.

4 Discussion

4.1 *Influence of particle on the partition of ^{210}Po and ^{210}Pb*

The ZCC contains plenty of riverwater from the Changjiang River (Yangtze River), Qiantang River, Oujiang River, Minjiang

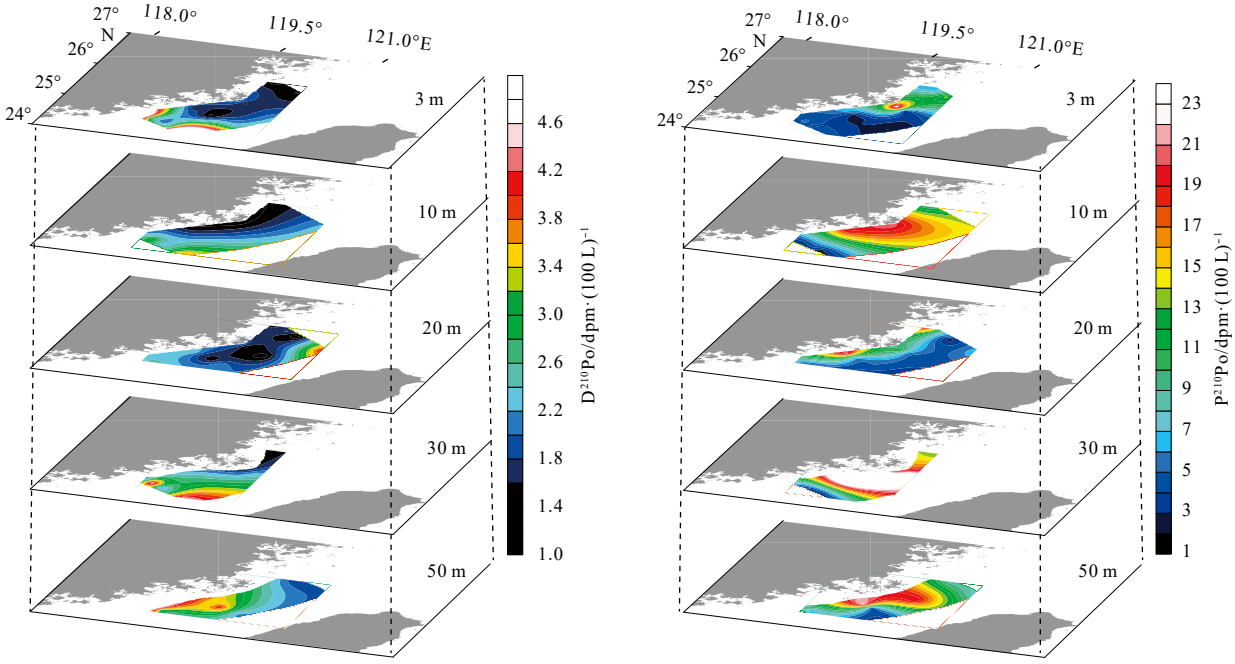

Fig. 3. Distributions of dissolved and particulate ^{210}Po in the Taiwan Strait in February 2012.

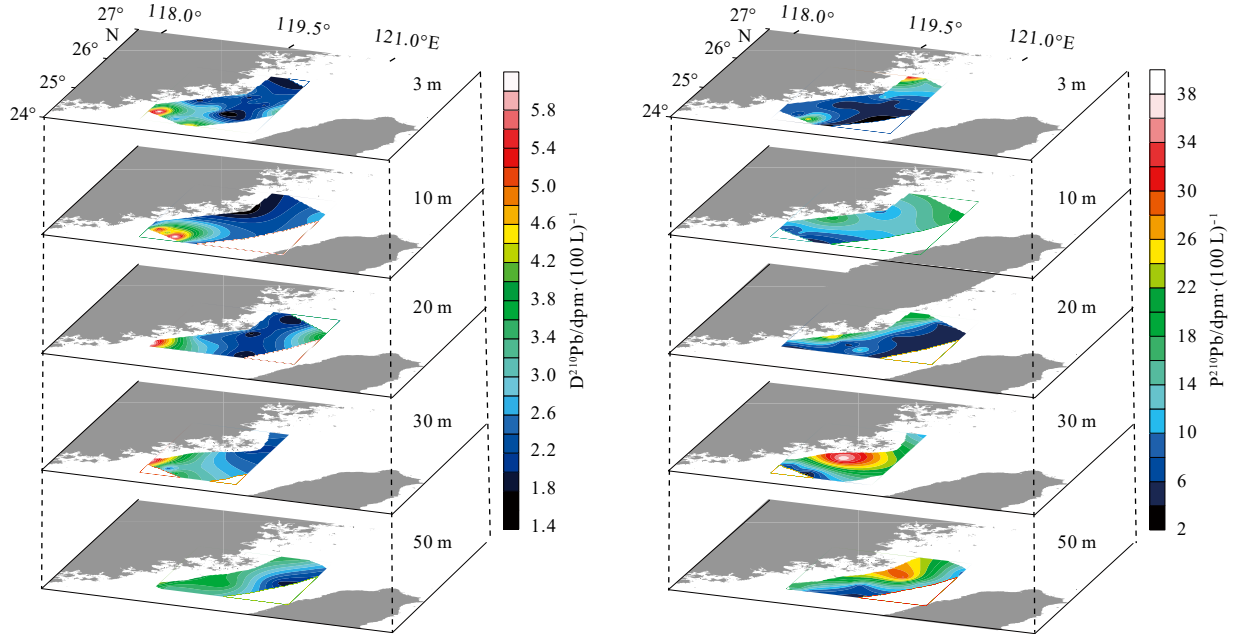

Fig. 4. Distributions of dissolved and particulate ^{210}Pb in the Taiwan Strait in February 2012.

River and Jiulong River. A large amount of terrestrial particulate matters and nutrients discharged into the ZCC usually benefit phytoplankton growth along the coast and might lead to high biogenic particle contents in this area. Owing to their particle-reactivity, ^{210}Po and ^{210}Pb are ready to be absorbed onto particles. The enriched particulate matter in the ZCC may result in difference in the partition of both ^{210}Po and ^{210}Pb between dissolved and particulate phases.

As shown in Table 1, the average partition coefficients of ^{210}Po and ^{210}Pb in the ZCC were 0.57 L/mg and 0.55 L/mg, respectively. By contrast, the averages of $K_{d,\,Po}$ and $K_{d,\,Pb}$ in the TWC were 0.92 and 1.53 L/mg. It is obvious that there is discernible difference in the K_d values between the ZCC and TWC. There are significant linear correlations between TPM contents and K_d values (Table 2), suggesting that particulate matters indeed control the partition of both ^{210}Po and ^{210}Pb in the Taiwan Strait. In addition, $K_{d,\,Po}$ significantly correlated with $K_{d,\,Pb}$ in the ZCC and TWC with different relationships between the two water masses (Fig. 6). The fractionation coefficients, averaging 1.17 in the ZCC, implied that particles seemed to preferably absorb ^{210}Po to ^{210}Pb. In comparison, particles in the TWC are likely to scavenge ^{210}Pb prior to ^{210}Po with the fractionation coefficient of 0.25. Such a difference is ascribed to the abundant biogenic particulate matters in the ZCC, probably induced by the amount of riverine nutrients. Bio-

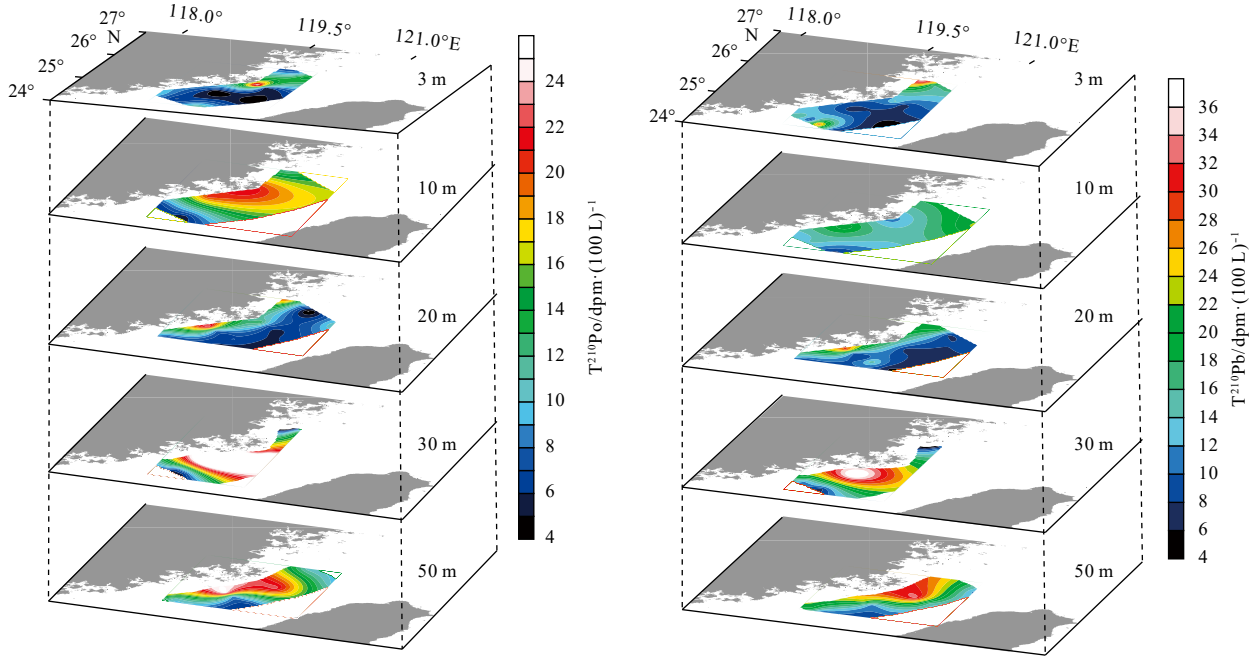

Fig. 5. Distributions of total ^{210}Po and total ^{210}Pb in the Taiwan Strait in February 2012.

Table 2. Correlations among TPM, P^{210}Po, P^{210}Pb, $K_{d,\,Po}$ and $K_{d,\,Pb}$ in the Zhemin Coastal Current (ZCC) and the Taiwan Warm Current (TWC)

		P^{210}Po	P^{210}Pb	$K_{d,\,Po}$	$K_{d,\,Pb}$
ZCC	TPM	0.393	0.710**	–0.414	–0.595**
	p (2-tailed)	0.096	0.001	0.078	0.007
	n	19	19	19	19
TWC	TPM	0.585**	0.456*	–0.427*	–0.421*
	p (2-tailed)	0.003	0.025	0.037	0.041
	n	24	24	24	24

Note: ** The correlation coefficient with 99% of confidence level (two-tailed test); * the correlation coefficient with 95% of confidence level (two-tailed test).

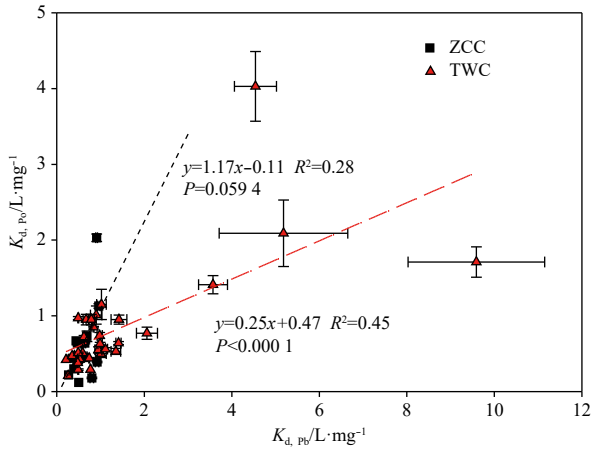

Fig. 6. Correlations between $K_{d,\,Po}$ and $K_{d,\,Pb}$ in the ZCC and TWC in February 2012.

genic particles usually contain plentiful organic compounds than terrestrial particles. Studies suggested that particle types with different chemical composition could lead to fractionation between ^{210}Po and ^{210}Pb (Yang et al., 2013, 2015). Thus, these results provided *in situ* evidence for the important role of particle composition in controlling the partition of ^{210}Po and ^{210}Pb between seawater and particles.

Further, the correlations between P^{210}Po or P^{210}Pb values and TPM contents lend supports to the important role of particles in scavenging ^{210}Po and ^{210}Pb. As shown in Fig. 7, activity concentrations of particulate ^{210}Po and ^{210}Pb in the TWC increased with the increasing TPM contents, indicating more particles would result in more ^{210}Po adsorption on particulate matter (Fig. 8). Similar scenarios were also observed in the ZCC. Hence, ^{210}Po and ^{210}Pb could be used to trace the cycling of particles in the Taiwan Strait.

4.2 *Particle sinking flux based on ^{210}Po/^{210}Pb*

Based on the close relations between ^{210}Po, ^{210}Pb and TPM, particle sinking was estimated in the Taiwan Strait. Using the one-dimensional irreversible model (Bacon et al., 1976), the variability in the amount of ^{210}Po (i.e., inventory) with time can be expressed as

$$\frac{\mathrm{d}I_{Po}}{\mathrm{d}t} = \lambda_{Po}\left(I_{Pb} - I_{Po}\right) + F_{atm.Po} - F_{Po}, \tag{3}$$

where I_{Po} and I_{Pb} represent the inventories of ^{210}Po and ^{210}Pb in the water column (dpm/m^2), λ_{Po} represents the decay constant of ^{210}Po (0.005 d^{-1}), $F_{atm.Po}$ is the atmospheric deposition flux of ^{210}Po (dpm/(m^2·d)), and F_{Po} denotes the sinking flux of the total ^{210}Po. Recent researches suggested that the residence time of ^{210}Po in the Taiwan Strait, calculated using the depositional flux ratio of ^{210}Po to ^{210}Pb, was less than half a month above the Taiwan Strait (Wang et al., 2014b; Wei et al., 2012). Therefore, atmospheric ^{210}Po deposition of (2.46±0.22) dpm/(m^2·d) within 15 d before sampling was adopted in the west coast of the Taiwan Strait (Zhang, 2015). F_{Po} is the sinking or export flux of ^{210}Po out of the water column; positive F_{Po} values represent a net sinking and negative F_{Po} would denote a net resuspension of sediment.

The export fluxes of ^{210}Po were presented in Table 3 and Fig. 9.

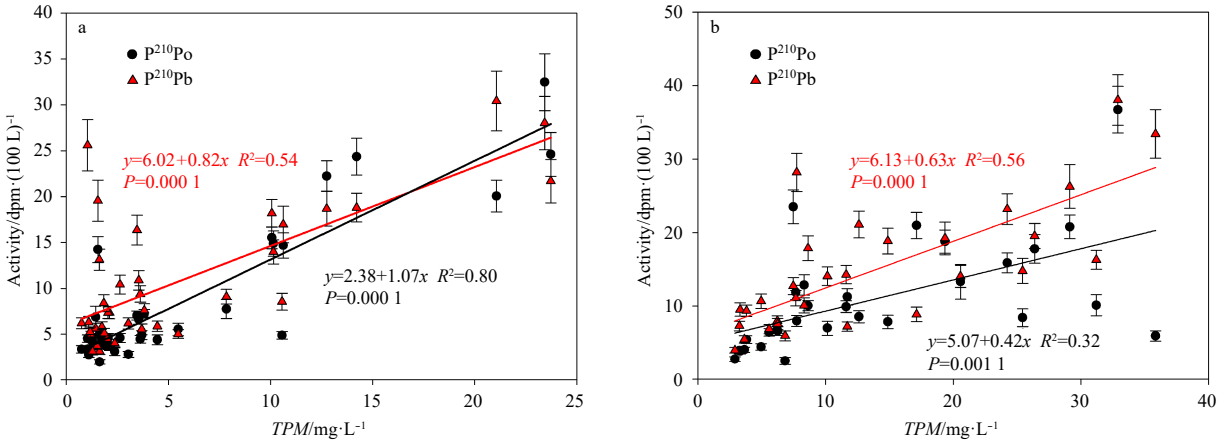

Fig. 7. Correlations between TPM and $P^{210}Po$ (or $P^{210}Pb$) in Taiwan Warm Current (a) and Zhemin Coastal Current (b).

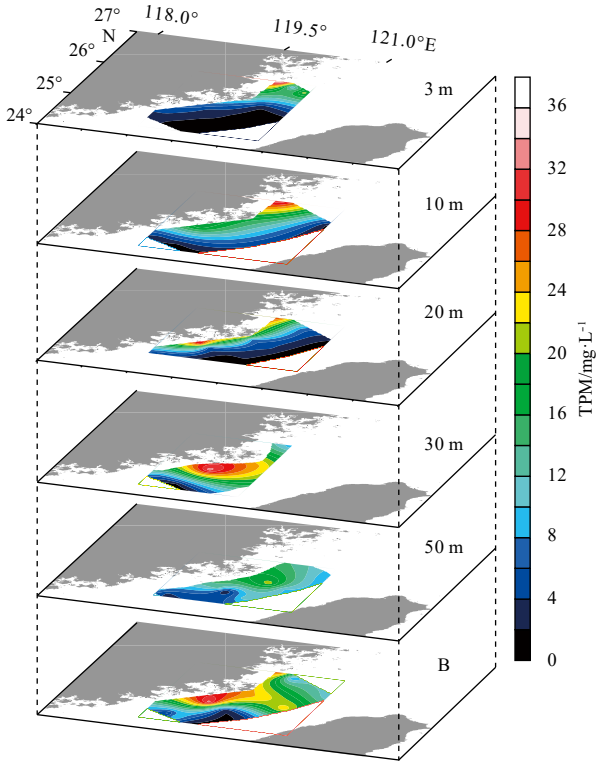

Fig. 8. Distributions of TPM in the Taiwan Strait in February 2012.

In general, ^{210}Po fluxes showed inhomogeneous distribution in the study area. Higher values occurred in the northern and southwest areas. The lowest values were observed around the Pingtan Island with no net sinking of ^{210}Po. Stations close to Taiwan also showed relatively low ^{210}Po fluxes. Since the total ^{210}Po decreased gradually during the TWC transport from the south to north in the Taiwan Strait (Table 1), the spatial patterns of ^{210}Po sinking revealed the continuous deposition of ^{210}Po along the TWC transport. The export of ^{210}Po could be used to constrain the sedimentation of particles.

To examine the details of ^{210}Po removal at different depths, the removal rates of ^{210}Po at each sampling depth were calculated based on the mass-balance model (Yang et al., 2006). As shown in Fig. 10, sinking of ^{210}Po out of the upper 20 m water column showed a similar pattern to the ^{210}Po fluxes out of the whole water column (Fig. 9), indicating that the removal of ^{210}Po mainly occurred in the upper 20 m water in the Taiwan Strait during winter.

Based on the hypothesis that TPM has the same residence time as $P^{210}Po$ (Eppley, 1989), we could calculate the sinking flux of TPM out of the water column via ^{210}Po:

$$F_{\mathrm{TPM}(\tau)} = F_{\mathrm{PPo}} \times \frac{I_{\mathrm{TPM}}}{I_{\mathrm{PPo}}}, \tag{4}$$

where $F_{\mathrm{TPM}(\tau)}$ (g/(m²·d)) represents the sinking flux of TPM out of the whole water column, I_{TPM} and I_{PPo} are the inventories of TPM and PPo, respectively. F_{PPo} (dpm/(m²·d)) is the flux of $P^{210}Po$, and $I_{\mathrm{TPM}}/I_{\mathrm{PPo}}$ denotes the inventory ratio of TPM to $P^{210}Po$. Results showed the sinking flux of TPM ranged from –0.22 to 3.84 g/(m²·d)

Table 3. Export fluxes of ^{210}Po and TPM in the Taiwan Strait in February 2012

Sampling ID	Export depth/m	F_{Po}/ dpm·m⁻²·d⁻¹	$F_{\mathrm{TPM}(\tau)}$/ g·m⁻²·d⁻¹	$F_{\mathrm{TPM(R)}}$/ g·m⁻²·d⁻¹
Y41	35	24.50±4.14	2.58±0.45	2.87±0.54
Y42	50	12.17±2.08	1.05±0.15	1.04±0.19
Y43	59	21.79±2.43	1.32±0.20	1.17±0.16
Y44	65	16.29±2.75	0.83±0.21	1.06±0.20
Y45	28	3.06±0.74	0.11±0.02	0.13±0.03
Y31	20	4.76±3.82	0.54±0.41	0.67±0.54
Y32	40	5.52±6.50	0.49±0.45	0.49±0.58
Y33	70	0.65±5.08	0.04±0.30	0.04±0.30
Y34	55	17.23±2.26	0.61±0.12	0.77±0.14
Y35	59	6.70±1.18	0.81±0.14	1.45±0.28
Y21	16	–2.03±0.99	–0.22±0.13	–0.62±0.31
Y22	41	0.70±3.62	0.16±0.57	0.11±0.55
Y23	30	2.45±1.71	0.23±0.17	0.23±0.17
Y24	48	14.52±7.95	1.45±0.63	1.52±0.85
Y25	64	2.07±4.36	0.13±0.28	0.15±0.31
Y11	25	14.52±3.80	3.84±0.32	2.15±0.25
Y12	40	16.05±3.43	2.18±0.52	1.04±0.25
Y13	48	17.84±3.44	3.11±0.63	2.63±0.57
Y15	75	7.50±3.92	0.41±0.25	0.54±0.29

Note: $F_{\mathrm{TPM}(\tau)}$: assuming the same residence time of TPM and particles in the water column; $F_{\mathrm{TPM(R)}}$: based on the ratio of TPM to ^{210}Po in particles.

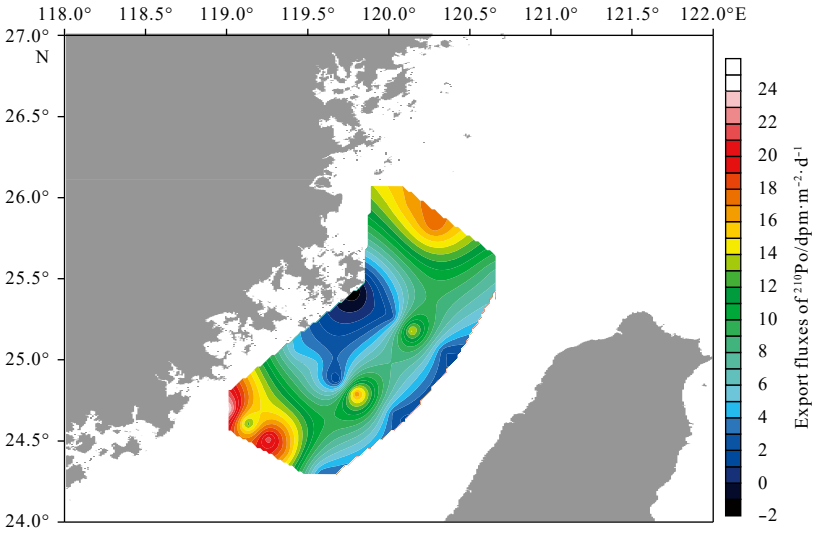

Fig. 9. Export fluxes of ^{210}Po in the Taiwan Strait in February 2012.

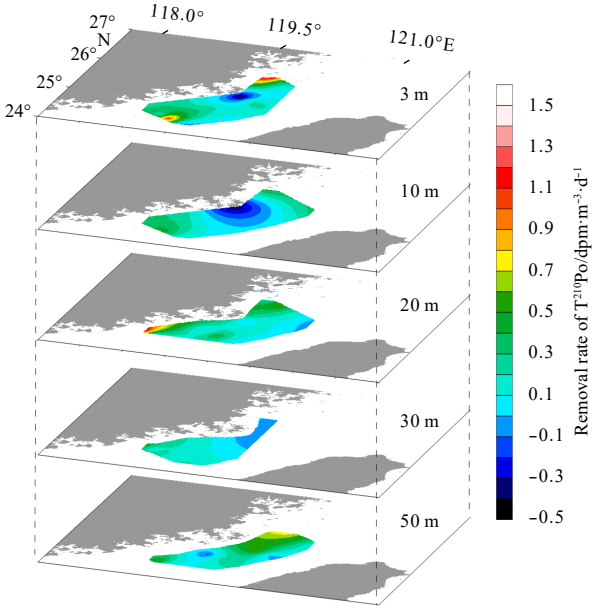

Fig. 10. Spatial pattern of the removal rate of T^{210}Po in the Taiwan Strait in February 2012.

with a mean value of 1.04 g/(m^2·d) (Table 3). Using the ratio of TPM content to P^{210}Po content (*PPo*) at the export depth, the sinking flux of TPM can also be estimated (Buesseler et al., 1992):

$$F_{\mathrm{TPM(R)}} = F_{\mathrm{Po}} \times \frac{TPM}{PPo}, \tag{5}$$

where $F_{\mathrm{TPM(R)}}$ is the sinking flux of TPM. $F_{\mathrm{TPM(R)}}$ varied from –0.62 to 2.87 g/(m^2·d), comparable to $F_{\mathrm{TPM(\tau)}}$ (Fig. 11) . Statistically, there is not difference between the two approaches (t-test, p>0.05). Our results were lower, to a varying degree, than the sediment accumulation rates of 3.29–47.95 g/(m^2·d) obtained using excess ^{210}Pb in sediments (Fig. 12) in the Taiwan Strait (Huh et al., 2011). The phenomenon revealed that particle sinking in winter is less efficient than some other seasons in the Taiwan Strait, probably owing to the low primary productivity and strong mixing of seawater in winter. In some other seasons, TPM sinking fluxes would be much higher than the sediment accumulation rate to compensate the deficit of TPM sinking in winter.

4.3 *Sinking pattern of particles in the Taiwan Strait*

The spatial pattern of TPM sinking benefits our understanding of the sediment accumulation in the Taiwan Strait. Stations close to the Pingtan Island showed sediment resuspension with negative TPM fluxes (Fig. 11), indicating that this area is a source site of sediment for around areas in winter. Thus, winnowing and focusing of sediment might be an important mechanism of sediment redistribution in the Taiwan Strait. High sinking rate occurred in the northern strait connecting the ECS and the southwest of the study area close to land. The central strait represents a moderate sinking flux area (Fig. 11), showing a resemblance to the spatial pattern of sedimentation rate obtained via sediments in the Taiwan Strait (Fig. 12; Huh et al., 2011).

Notably, there are differences in the distribution patterns of particle sinking between our results and those from Huh et al. (2011) though both patterns showed an overall similarity (Figs 11 and 12). First, our results indicated a net resuspension at sites close to the Pingtan Island (around Sta. Y21) in winter; however, the long-term record (i.e., sediment accumulation) suggested that all the study stations are net particle sedimentation sites. Such a difference implied significant seasonal variability in both the sinking of particles and resuspension of sediments in the Taiwan Strait. In some seasons, the net effect of the two processes results in a net sedimentation of particle, while it shows a net resuspension in other seasons. Over a long timescale, particles showed a transport from the water column to sediment. Second, the sinking fluxes of particle seemed to be lower than the sedimentation accumulation rates (Huh et al., 2011). For example, the flux at Y12 was about 30% of the sedimentation rate obtained at the same site (OR2-1638-GC21 in Huh et al., 2011). The fluxes at Y23 and Y25 were about 2% of those sedimentation rates (Stas OR1-841-GC-14 and OR2-1442-GC29). Probably, the strong mixing in winter benefits the resuspension process and leads to a low sinking fluxes of particle. Considering the fact that inorganic minerals contribute the majority of the bulk particle regime, the lower sinking fluxes in winter indicated that the Taiwan

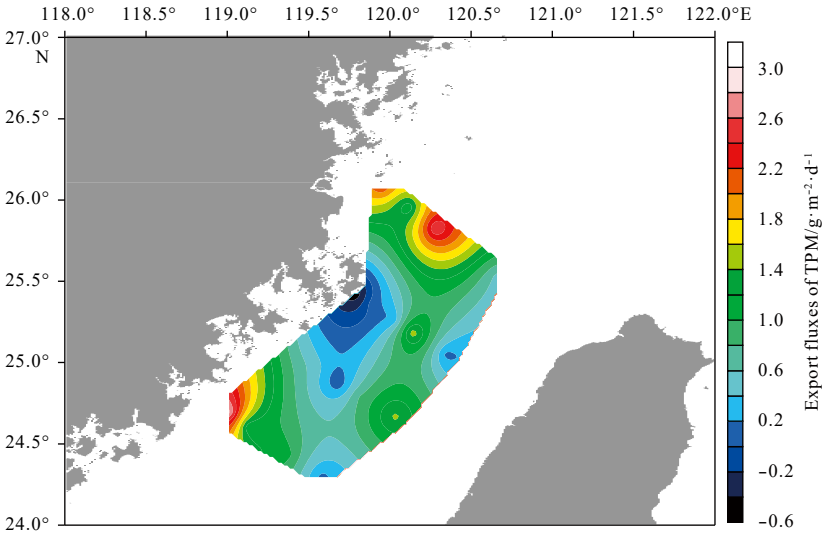

Fig. 11. Export fluxes of TPM in the Taiwan Strait.

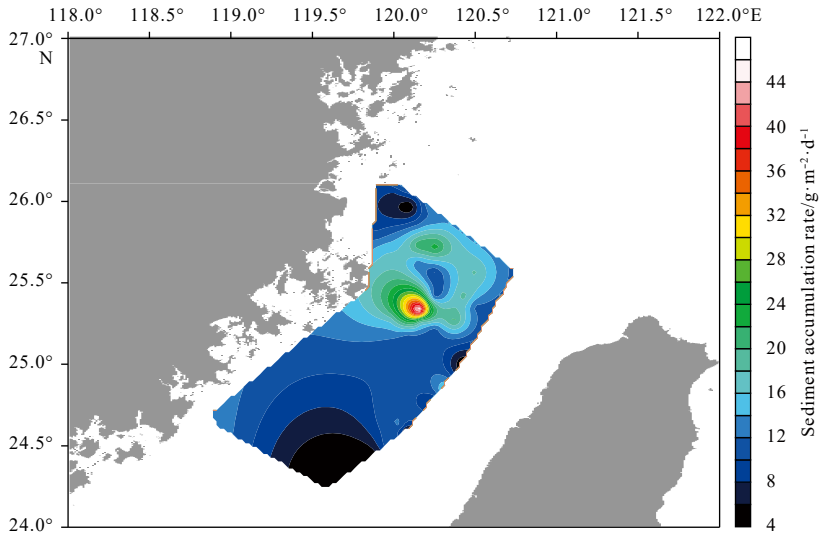

Fig. 12. Spatial pattern of sediment accumulation rate in the Taiwan Strait (data from Huh et al., 2011).

Strait might be an important source region of sediment for adjacent ECS. A large amount particulate matter probably transported to the ECS along the TWC in winter.

5 Conclusions

Distributions of ^{210}Po and ^{210}Pb revealed the important role of the ZCC and TWC in affecting their spatial characteristics in the Taiwan Strait. Particle composition, probably organics and minerals, greatly influences the fractionation between ^{210}Po and ^{210}Pb. In winter, the Taiwan Strait showed lower particle sinking fluxes comparing with some other seasons, indicating a significant seasonal variability in sedimentation and a transport of a large amount of particulate matter from the Taiwan Strait to the ECS. Thus, the intra-annual variations in the sinking of particles are crucial to our understanding of the material-balance in either the Taiwan Strait or the ECS.

Acknowledgements

We appreciate the insightful suggestions from two anonymous reviewers and Zongqiang Zhu in Guilin University of Technology. We also thank the laboratory staff and the crew of R/V *Yanping II* for their help during sampling and analysis.

References

Bacon M P, Spencer D W, Brewer P G. 1976. ^{210}Pb/^{226}Ra and ^{210}Po/^{210}Pb disequilibria in seawater and suspended particulate matter. Earth and Planetary Science Letters, 32(2): 277–296, doi: 10.1016/0012-821X(76)90068-6

Buesseler K O, Bacon M P, Cochran J K, et al. 1992. Carbon and nitrogen export during the JGOFS North Atlantic Bloom experiment estimated from ^{234}Th:^{238}U disequilibria. Deep Sea Research Part A. Oceanographic Research Papers, 39(7–8): 1115–1137, doi: 10.1016/0198-0149(92)90060-7

Chen Min, Ma Qiang, Guo Laodong, et al. 2012. Importance of lateral transport processes to ^{210}Pb budget in the eastern Chukchi Sea during summer 2003. Deep Sea Research Part II: Topical Studies in Oceanography, 81–84: 53–62, doi: 10.1016/j.dsr2.2012.03.011

Eppley R W. 1989. New production: history, methods, problems. In: Berger W H, Smetacek V S, Wefer G, eds. Productivity of the Ocean: Present and Past. New York: John Wiley and Sons, 85–97

Fang Ziming, Yang Weifeng, Zhang Xinxing, et al. 2013. Sedimenta-

tion and lateral transport of ^{210}Pb over the East China Sea shelf. Journal of Radioanalytical and Nuclear Chemistry, 298(2): 739–748, doi: 10.1007/s10967-013-2561-4

Fisher N S, Teyssié J L, Krishnaswami S, et al. 1987. Accumulation of Th, Pb, U, and Ra in marine phytoplankton and its geochemical significance. Limnology and Oceanography, 32(1): 131–142, doi: 10.4319/lo.1987.32.1.0131

Fowler S W. 2011. ^{210}Po in the marine environment with emphasis on its behaviour within the biosphere. Journal of Environmental Radioactivity, 102(5): 448–461, doi: 10.1016/j.jenvrad.2010.10.008

Hu Jianyu, Hong Huasheng, He Zhigang, et al. 1999. Vertical distribution features of temperature and salinity in the northern Taiwan Strait during February–March, 1998. Marine Sciences (in Chinese), (4): 51–54

Hu Jianyu, Kawamura H, Li Chunyan, et al. 2010. Review on current and seawater volume transport through the Taiwan Strait. Journal of Oceanography, 66(5): 591–610, doi: 10.1007/s10872-010-0049-1

Huh C A, Chen Weifang, Hsu F H, et al. 2011. Modern (<100 years) sedimentation in the Taiwan Strait: rates and source-to-sink pathways elucidated from radionuclides and particle size distribution. Continental Shelf Research, 31(1): 47–63, doi: 10.1016/j.csr.2010.11.002

Huh C A, Su C C. 1999. Sedimentation dynamics in the East China Sea elucidated from ^{210}Pb, ^{137}Cs and ^{239,240}Pu. Marine Geology, 160(1–2): 183–196, doi: 10.1016/S0025-3227(99)00020-1

Jones P, Maiti K, McManus J. 2015. Lead-210 and Polonium-210 disequilibria in the northern Gulf of Mexico hypoxic zone. Marine Chemistry, 169: 1–15, doi: 10.1016/j.marchem.2014.12.007

Li Yan, Chen Yining, Ruan Meina, et al. 2015. The Jiulong River plume as cross-strait exporter and along-strait barrier for suspended sediment: Evidence from the endmember analysis of in-situ particle size. Estuarine, Coastal and Shelf Science, 166: 146–152, doi: 10.1016/j.ecss.2015.03.002

Moore H E, Poet S E, Martell E A. 1973. ^{222}Rn, ^{210}Pb, ^{210}Bi, and ^{210}Po profiles and aerosol residence times versus altitude. Journal of Geophysical Research, 78(30): 7065–7075, doi: 10.1029/JC078i030p07065

Nozaki Y, Zhang Jing, Takeda A. 1997. ^{210}Pb and ^{210}Po in the equatorial Pacific and the Bering Sea: the effects of biological productivity and boundary scavenging. Deep Sea Research Part II: Topical Studies in Oceanography, 44(9–10): 2203–2220, doi: 10.1016/S0967-0645(97)00024-6

Shang Shaoling, Hong Huasheng, Shang Shaoping, et al. 2001. Intrusion of warm water into the Taiwan Strait during winter monsoon of 1998 and its ecological response. Journal of Remote Sensing (in Chinese), 5(5): 383–387

Sun Haowei. 2016. A study on the seasonal and interannual variations of kuroshio invasion into the Taiwan strait and its physical mechanism (in Chinese) [dissertation]. Xiamen: Third Institute of Oceanography, State Oceanic Administration

Wang Aijun, Ye Xiang, Du Xiaoqin, et al. 2014a. Observations of cohesive sediment behaviors in the muddy area of the northern Taiwan Strait, China. Continental Shelf Research, 90: 60–69, doi: 10.1016/j.csr.2014.04.002

Wang Zhou, Yang Weifeng, Chen Min, et al. 2014b. Intra-annual deposition of atmospheric ^{210}Pb, ^{210}Po and the residence times of aerosol in Xiamen, China. Aerosol and Air Quality Research, 14(5): 1402–1410, doi: 10.4209/aaqr.2013.05.0170

Wei C L, Chou L H, Tsai J R, et al. 2009. Comparative geochemistry of ^{234}Th, ^{210}Pb, and ^{210}Po: a case study in the Hung-Tsai Trough off south western Taiwan. Terrestrial Atmospheric and Oceanic Science, 20: 411–423, doi: 10.3319/TAO.2008.01.09.01(Oc)

Wei C L, Lin S Y, Sheu D D D, et al. 2011. Particle-reactive radionuclides (^{234}Th, ^{210}Pb, ^{210}Po) as tracers for the estimation of export production in the South China Sea. Biogeosciences, 8(12): 3793–3808, doi: 10.5194/bg-8-3793-2011

Wei C L, Chen P R, Lin S Y, et al. 2015. Distributions of ^{210}Pb and ^{210}Po in surface water surrounding Taiwan: a synoptic observation. Deep Sea Research Part II: Topical Studies in Oceanography, 117: 155–166, doi: 10.1016/j.dsr2.2014.04.010

Wei C L, Lin S Y, Wen L S, et al. 2012. Geochemical behavior of ^{210}Pb and ^{210}Po in the nearshore waters off western Taiwan. Marine Pollution Bulletin, 64(2): 214–220, doi: 10.1016/j.marpolbul.2011.11.031

Xiao Hui, Guo Xiaogang, Wu Risheng. 2002. Summarization of studies on hydrographic characteristics in Taiwan Strait. Journal of Oceanography in Taiwan Strait (in Chinese), 21(1): 126–138

Xu Maoquan, Chen Youfei. 1999. Geological Oceanography (in Chinese). Xiamen: Xiamen University Press

Yang Weifeng. 2005. Marine biogeochemistry of ^{210}Po and ^{210}Pb and their implications regarding the cycling and export of particles (in Chinese) [dissertation]. Xiamen: Xiamen University

Yang Weifeng, Huang Yipu, Chen Min, et al. 2006. Disequilibria between ^{210}Po and ^{210}Pb in surface waters of the southern South China Sea and their implications. Science in China Series D, 49(1): 103–112, doi: 10.1007/s11430-004-5233-y

Yang Weifeng, Huang Yipu, Chen Min, et al. 2011. Unusually high ^{210}Po activities in the surface water of the Zhubi Coral Reef Lagoon in the South China Sea. Science of the Total Environment, 409(21): 4612–4617, doi: 10.1016/j.scitotenv.2011.07.040

Yang Weifeng, Guo Laodong, Chuang C Y, et al. 2013. Adsorption characteristics of ^{210}Pb, ^{210}Po and ^{7}Be onto micro-particle surfaces and the effects of macromolecular organic compounds. Geochimica et Cosmochimica Acta, 107: 47–64, doi: 10.1016/j.gca.2012.12.039

Yang Weifeng, Guo Laodong, Chuang C Y, et al. 2015. Influence of organic matter on the adsorption of ^{210}Pb, ^{210}Po and ^{7}Be and their fractionation on nanoparticles in seawater. Earth and Planetary Science Letters, 423: 193–201, doi: 10.1016/j.epsl.2015.05.007

Zhang Lihao. 2015. Distribution patterns of ^{210}Po and ^{210}Pb and particle export in the Taiwan Strait (in Chinese) [dissertation]. Xiamen: Xiamen University

Zhou Dicheng. 1987. The distribution and controlling factors of submarine sediments in the west coastal Taiwan Strait. Haiyang Xuebao (in Chinese), 9(1): 64–68